World Conference on Timber Engineering Oslo 2023

PREDICTION OF DOUGLAS-FIR SAWN TIMBER YIELD BASED ON LOG COMPUTED TOMOGRAPHY

Andreas Weidenhiller[1], Boris Sandor[2], Thomas Simlinger[3], Franka Brüchert[4], Johannes A. J. Huber[5]

ABSTRACT: Climate change affects the growth conditions for Norway spruce (*Picea abies*) which is the most important species for the European construction timber industry. As a countermeasure, the species mix in European forests is being changed to include more hardwood, but also more drought-resistant softwood species, for example Douglas-fir (*Pseudotsuga menziesii*). Previous research has shown that Douglas-fir can on the one hand be suitable to produce high-strength material. On the other hand, however, Douglas-fir wood can also have a considerably lower strength than what is expected from spruce. Therefore, there is need for improved strength prediction and strength grading methods for Douglas-fir, to enable the correct allocation of Douglas-fir roundwood to the most suitable target product. In the present study, computed tomography (CT) image reconstructions of 53 Douglas-fir logs were used to predict the strength of the sawn timber and thus to identify logs which are suitable to produce glulam lamellas. To achieve this, statistical modelling was combined with Finite Element (FE) modelling of destructive tensile tests, based on simulated fibre orientations for the boards.

KEYWORDS: Douglas-fir (*Pseudotsuga menziesii*), strength prediction, glulam lamellas, statistical modelling, simulated fibre orientations, Finite Element Analysis

1 INTRODUCTION

Europe aims to proceed towards a sustainable bio-based economy, which should be less dependent on fossil resources [1]. Forest based products, including construction timber products, are an important element in this strategy. At the same time, the growth conditions are declining for spruce (*Picea abies*) which is Europe's most important wood species for construction timber products – due to climate change, temperatures are rising, and the risk of drought is increasing. Douglas-fir (*Pseudotsuga menziesii*) is seen as one of the tree species which could complement spruce in the future, due to its drought resistance, fast growth and interesting material properties [2]. Sauter [3], e.g., observed an average tensile strength of more than 40 N/mm², but with unusually high coefficients of variation (CoV) of 50%-60%. Rais et al. [4] reported, for material from a plant density trial, average tensile strengths between 17 N/mm² and 25 N/mm² with CoV in the range of 30%-40%. Such high variations in sawn timber properties can be a challenge for the construction timber industry. Therefore, our study presents methods to predict the sawn timber strength already at the roundwood stage and thus to allow identification of suitable raw material for glulam production.

2 MATERIAL AND METHODS

2.1 MATERIAL

For this study, 53 Douglas-fir logs from two stands (age of 60 years) close to Vienna (Austria) were selected, focusing on qualities which are typically used for construction timber production. The share of quality class A according to Austrian wood trade practices was 9%, that of quality class B 76%. 15% of the wood corresponded to the quality class C. The roundwood diameters were between 25 cm and 46 cm.

2.2 ROUNDWOOD SCANNING AND SAWING

The logs were scanned with the roundwood CT scanner at the Forest Research Institute Baden-Württemberg in Freiburg, Germany. Based on the CT image reconstruction, several wood properties were extracted, among them heartwood, knots and pith. For the knots, parametric descriptions similar to Johansson et al [5] were computed.

[1] Andreas Weidenhiller, Holzforschung Austria, Franz-Grill-Straße 7, Vienna, Austria, a.weidenhiller@holzforschung.at
[2] Boris Sandor, Holzforschung Austria, Austria, b.sandor@holzforschung.at
[3] Thomas Simlinger, Holzforschung Austria, Austria, th.simlinger@gmail.com
[4] Franka Brüchert, Forest Research Institute Baden-Württemberg, Germany, franka.bruechert@forst.bwl.de
[5] Johannes A. J. Huber, Luleå University of Technology, Sweden, johannes.huber@ltu.se

https://doi.org/10.52202/069179-0105

Further, the longitudinal eigenfrequency f of each log was measured using a Microtec ViScan device, and the dynamic modulus of elasticity $E_{dyn,log}$ was calculated for each log using Equation (1):

$$E_{dyn,log} = 4 \cdot \rho_{log} (l \cdot f)^2 \quad (1)$$

Where ρ_{log} was the average log density from CT scanning and l was the log length.
The logs were sawn according to the cutting patterns given in Figure 1. 14 logs were sawn according to pattern a, 23 logs according to pattern b, and 16 logs according to pattern c. One log in pattern c was accidentally sawn so that it had four more side boards. In total, sawing yielded 267 main boards and 156 side boards. The boards were dried to a target moisture content (MC) of 12%. The main boards were planed to a thickness of 45 mm; the side boards were all planed to a thickness of 25 mm.

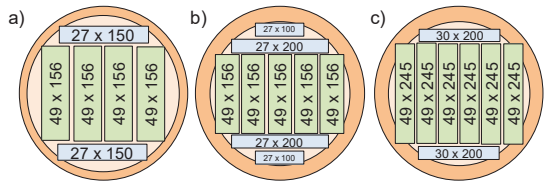

Figure 1: *Cutting patterns used for sawing the Douglas fir logs (board dimensions in mm). One of the logs in pattern c had 4 additional side boards of the dimensions 30 x 100 mm².*

2.3 SAWN TIMBER SCANNING AND TESTING

After planing, the boards were strength graded with a Microtec GoldenEye 706 machine including X-ray and eigenfrequency measurement. At the laboratory of Holzforschung Austria, the boards underwent destructive tensile testing according to EN 408 [6], including measurement of dry wood density and MC on a small clear sample of each tested board, and corrections of the values according to EN 384 [7]. However, it was decided to exclude the 28 side boards of dimension 27x150 mm² from destructive testing, as their number was so small.
Further, 14 main boards and 14 side boards had to be excluded due to various reasons, like breakage during machine strength grading or excessive wane.
The final yield was: 253 main boards with the cross sections 45x145 mm² and 45x230 mm², and 104 side boards with 25x90 mm² and 25x185 mm².

2.4 TRACKING OF TIMBER POSITIONS

The position of each board in the respective log was tracked using log end templates [8]. Those templates were sheets of paper containing the log ID as well as angular information and distance to the pith (see Figure 2a). The sheets were glued to one log end and remained there during sawing, drying, planing, industrial strength grading and destructive testing (Figure 2b). At the end of the process, the templates on the boards were scanned and manually arranged to reconstruct the original positions of the then dry boards in the green log CT reconstruction. To easily arrange the images, a dedicated tool was programmed by the authors (Figure 2c) using R [9] and the shiny package [10].

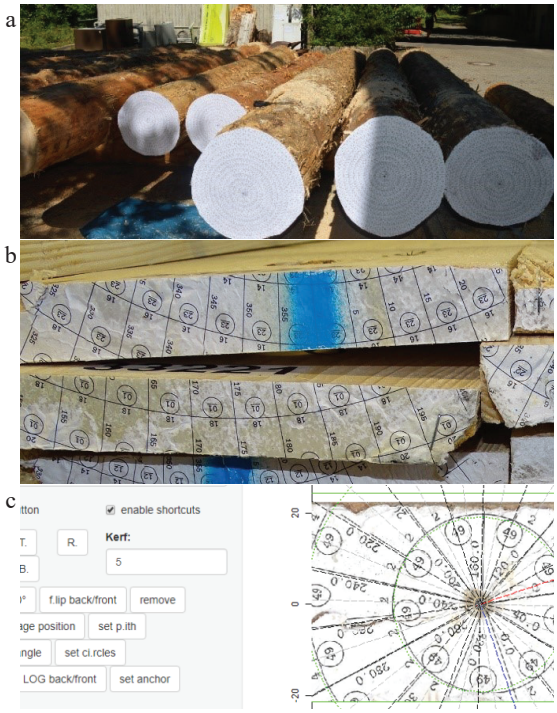

Figure 2: *Log end templates. a) glued to the log end, b) remaining on the board throughout the board processing, c) detail screenshot of the tool to arrange the scans.*

2.5 VIRTUAL SAWING

Using the reconstructed board positions, virtual boards were created from the CT images of the log. For each virtual board, descriptive variables were calculated, including heartwood density, distance from pith and percentage of knot volume. Further, a board X-ray scan was simulated by calculating average densities along the direction of the board thickness, which resulted in density data arrays of the dimensions “board width” by “board length”. These green densities were assumed to have been measured at an MC of $u = 29\%$ (fibre saturation point) and were corrected to an MC of $u_{\text{ref}} = 12\%$ using Equation (2) (EN 384 [7]).

$$\rho = \rho(u)\big(1 - 0.005(u - u_{\text{ref}})\big) \quad (2)$$

2.6 SIMULATION OF FIBRE ORIENTATIONS

Based on the parametric knot descriptions calculated on the CT images and using the reconstructed board position, fibre orientations were simulated along the length and width of the central plane for each board at a resolution of one grid point per mm, using the approach described by Huber et al. [11]. A detail of such reconstructed fibre

https://doi.org/10.52202/069179-0105

orientations is shown in Figure 3. For the figure, the resolution was reduced to one grid point per 5mm.

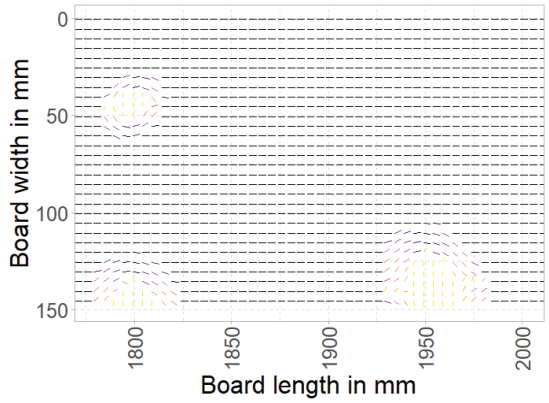

Figure 3: *Detail of simulated fibre orientations: flow of fibres around three knots in board 23047. Each line segment corresponds to one grid point, colours indicate the magnitude of the grain deviation.*

2.7 FINITE ELEMENT MODEL

Using COMSOL Multiphysics® [12], tensile tests were simulated on a two-dimensional plane stress model of each board. The calculated fibre orientations (section 2.6) were used to generate a locally varying coordinate system. This system transforms the three-dimensional cylindrical (LRT) material properties defined by the reference stiffness tensor C [13] to the two-dimensional model of the board – see Equation (3).

$$C(\rho) = \frac{\rho(x,y)}{\rho_{ref}} \begin{bmatrix} 11162 & 504 & 435 & 0 & 0 & 0 \\ & 866 & 281 & 0 & 0 & 0 \\ & & 528 & 0 & 0 & 0 \\ & & & 620 & 0 & 0 \\ & sym & & & 500 & 0 \\ & & & & & 23 \end{bmatrix} \quad (3)$$

Due to the density dependence of this stiffness tensor the local values were linearly scaled from the reference density of $\rho_{ref} = 390$ kg/m³ according to the local density $\rho(x,y)$ obtained from the virtual board (section 2.5). The discretization was performed with a uniform quadrilateral mesh with a resolution of 1 mm. In order to determine the Young's Modulus one side of the board was constrained in both spatial directions while the other side was prescribed a displacement of 5 mm along the x-axis. From the reaction forces, the Young's Modulus was calculated for each board.

2.8 MODELLING THE SAWN TIMBER STRENGTH GRADING

We wanted to predict the grade yield achieved by the GoldenEye 706 sawn timber strength grading machine. For this purpose, we modelled the GoldenEye Indicating Property (IP) for strength with linear regression, based on descriptive variables extracted from the virtual boards, the Young's Modulus from the FE model, as well as the $E_{dyn,log}$ in various combinations. The regression coefficients were calculated on the training data set, which encompassed 60% of the logs in the study (33 logs, 208 boards). The following predictors for the GoldenEye 706 strength IP were calculated:

- VB ("virtual board") using the virtual board's knottiness, heartwood density and distance to pith information (section 2.2);
- VB+FE, using in addition the Young's Modulus from the FE model (section 2.7);
- VB+Edyn,log, which combined the virtual board's knottiness and heartwood density with the $E_{dyn,log}$ (section 2.2).

2.9 YIELD PREDICTION

For the GoldenEye strength IP, a setting S for strength grading into strength class T14 was calculated on the training set, using a simplified approach based on EN 14081-2 [14]. The T14 strength class is defined in EN 338 [15] with the following properties: 5th percentile of tensile strength ($f_{t,k}$) at least 14 N/mm²; average tensile modulus of elasticity ($E_{t,0,mean}$) at least 11 kN/mm², and fifth percentile of the density (ρ_k) at least 350 kg/m³. T14 is one of the most important strength classes for producing glue laminated timber (glulam) of strength class GL24h [16].

Boards with an IP below the setting value S were rejected, and all other boards were assigned to T14. The same setting S was applied to the three IP predictors calculated on the log scanning data (section 2.8). This was used to predict the yield of T14 boards from the sawn timber strength grading.

2.10 LOG PRESORTING

Log pre-sorting was done by assigning only such logs to the production of T14 boards where the predicted yield was above a certain threshold T, which we varied from 0% to 100%.

The efficiency of the pre-sorting was defined as obtaining as many T14 boards as possible from the given logs while producing as few rejected boards during the sawn timber strength grading as possible.

This trade-off was visualised using the following two quantities in Equations (4) and (5).

$$total\ yield\ T14 = \frac{n_{T14,grading}}{n_{boards,sawn}} \quad (4)$$

$$relative\ yield\ T14 = \frac{n_{T14,grading}}{n_{boards,grading}} \quad (5)$$

where $n_{T14,grading}$ means the number of boards assigned to T14 during strength grading, $n_{boards,sawn}$ means the number of all boards sawn from all logs, and $n_{boards,grading}$ means the number of boards sent to the strength grading process. Thus, the $total\ yield\ T14$ is the percentage of T14 boards relative to the number of all

https://doi.org/10.52202/069179-0105

boards sawn from all logs, and the $relative\ yield\ T14$ is the percentage of T14 boards relative to the number of boards sent to strength grading.

To get a more complete picture, the whole range of pre-sorting thresholds was calculated, which resulted in a curve of values in the diagram $total\ yield\ T14$ vs. $relative\ yield\ T14$. These curves were compared between the three predictors VB, VB+FE and VB+Edyn,log.
Finally, the curves for each predictor were compared to those obtained on the test dataset, which encompassed 40% of the logs in the study (20 logs, 149 boards). Similar curves between training and test are an indication that the pre-sorting approach could also work on future unknown data.

2.11 CALCULATIONS AND VISUALISATION

All calculations were done with R 4.2.1 [9]. The diagrams were created in R using the ggplot2 package version 3.4.0 [17].

3 RESULTS AND DISCUSSION

3.1 FINITE ELEMENT SIMULATIONS

In Figure 4, the Young's modulus calculated by the FE models was compared to the modulus of elasticity determined during the destructive tensile tests. We observed a moderate correlation with a coefficient of determination of $r^2 = 0.46$.

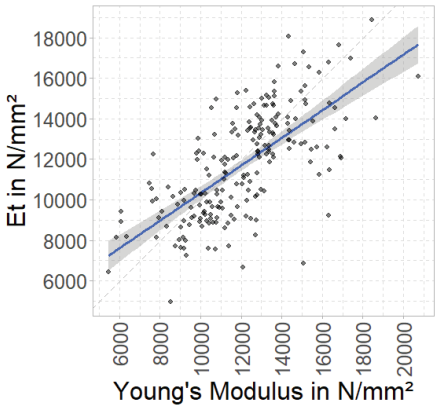

Figure 4: *The Young's modulus obtained from the FE models against the modulus of elasticity* $\boldsymbol{E_t}$ *from the destructive tensile tests for the 208 boards from the training dataset; coefficient of determination* $\boldsymbol{r^2 = 0.46}$.

For comparison: Olsson et al [18] achieved up to $r^2 = 0.70$ of their models with local modulus of elasticity in bending, $r^2 = 0.80$ if they included density, and $r^2 = 0.84$ if they included the longitudinal dynamic modulus of elasticity of the board ($E_{dyn,board}$).
When we used a two-dimensional density array measured on the dry boards during industrial strength grading (section 2.3), the coefficient of determination increased from 0.46 to 0.52, but this information is never available at the log stage. In other words, the knowledge of the boards' dry density improved the FE model – therefore, it would be desirable to develop an improved prediction of the dry density based on the green density.
Also, $E_{dyn,board}$ is never available at the log stage. However, a linear regression model for E_t, based on the Young's modulus from the FE model and on $E_{dyn,log}$ led to an $r^2 = 0.67$. Therefore, we also looked at yield prediction models including $E_{dyn,log}$, even though this quantity is not used in practice in Europe – for logs in intermediate states between frozen and thawed, $E_{dyn,log}$ cannot be determined reliably [19].
A further possibility for improving the prediction of the Young's modulus would be to base the FE model on a three-dimensional grid of fibre orientations instead of on a two-dimensional grid. This is planned as a next step in our research.

3.2 YIELD PREDICTION

Each of the three predictors predicted the correct grade for about 85% of the boards in the training data, with a clear tendency to overestimate the number of T14 boards – between 60% and 70% of the wrongly predicted boards were rejected boards which were assigned to T14 by the predictors.

3.3 LOG PRESORTING

In Figure 5, the *relative yield* was plotted against the *total yield* of T14 boards from the training data. This resulted in three curves for the three yield predictors VB, VB+FE and VB+Edyn,log. In the background of Figure 5, also the curve resulting from perfect yield prediction is displayed as a thin grey line.

An increase in the relative yield could only be achieved at the cost of a decrease in the total yield.

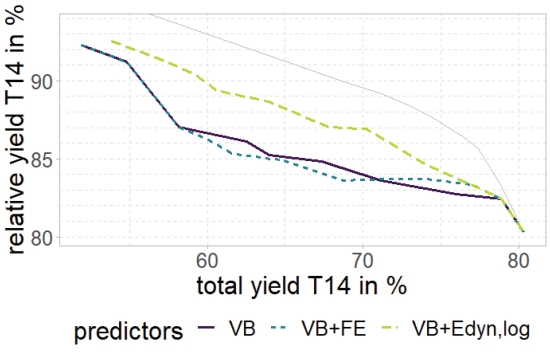

Figure 5: *Relative yield vs. total yield for the three yield predictors VB, VB+FE and VB+Edyn,log, based on the 208 boards from the training data. The thin grey curve to the right is the best possible pre-sorting, resulting from perfect foreknowledge of the final grading result.*

https://doi.org/10.52202/069179-0105

In Figure 5, this is apparent because the curves all decrease from left to right, even the thin grey line based on perfect yield prediction.
This trend is directly related to the pre-sorting strategy (section 2.10). We excluded logs with a predicted yield of T14 which was below a certain threshold *T*. A low predicted yield of T14 means a high predicted number of reject boards. Excluding these logs meant that the logs chosen to produce T14 boards had a lower share of reject and a higher share of T14, i.e. a higher relative yield. However, even from logs with a low yield of T14, we would be able to produce some T14 boards. When those logs were excluded based on the yield threshold *T*, those T14 boards could not be produced, and the total number of produced T14 boards decreased. This implied a lower total yield of T14.
When comparing the curves for the three yield predictors, curves further to the right (i.e., with a higher total yield for any given relative yield) indicate a higher pre-sorting efficiency, because this means that a given relative yield can be achieved while maintaining a higher total yield. Therefore, the thin grey line based on a perfect yield prediction is always furthest to the right. In Figure 5, the curve of the predictor VB+Edyn,log was closest to the perfect prediction curve and thus had the highest pre-sorting efficiency. We had expected that the predictor VB+FE would have a higher pre-sorting efficiency than VB, but, in fact, those two predictors were at the same level. It seems that a more accurate FE simulation of the Young's Modulus is needed to improve the pre-sorting efficiency, for example by basing the FE model on a three-dimensional grid.
In Figure 6, the yield curves were compared between the training data and the test data separately for each predictor. For all three predictors, the training data and the test data led to similar curves, given the rather small number of logs involved. Therefore, the pre-sorting strategies defined in this study should also work on new unknown data, although a repetition of the present study on a larger data set is recommended.

In Table 1, some selected value combinations of total yield and relative yield were extracted from Figure 6. Further, the values for the perfect prediction (as if one knew the result from board strength grading already when pre-sorting the logs) were added. To get a total yield value for a certain given relative yield value for all predictors, the total yield values were linearly interpolated between data points.
A relative yield of 80% was the baseline, where no logs were excluded. Therefore, all predictors had a total yield of 80% for this row. In the test data, this corresponded to 119 T14 boards and 30 reject boards.
A relative yield of 85% (test data), was achieved by the predictors VB and VB+FE at a total yield level of 66%. This corresponded to 99 T14 boards and 22 boards rejected during grading, but by excluding some logs, the opportunity to produce 20 more T14 boards was traded against having 13 less reject boards.

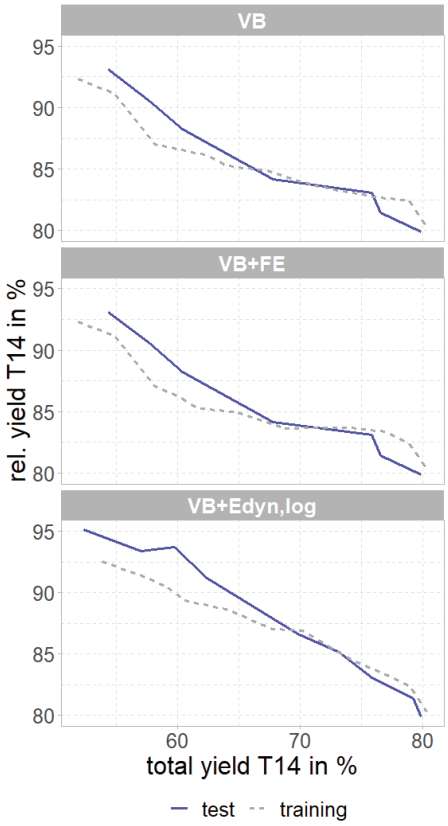

Figure 6: *The yield curves from Figure 5 (training data, 208 boards), compared to the curves resulting from the test data (149 boards).*

Table 1: *Interpolated values for the total yield at a certain level of relative yield for the different predictors and for the perfect prediction, for the training data and the test data.*

	relative yield in %	total yield in %			
		VB	VB+ FE	VB+ Edyn,log	perfect prediction
training (n = 208)	80	80	80	80	80
	85	66	64	73	78
	90	56	56	60	69
	92	52	52	55	62
test (n = 149)	80	80	80	80	80
	85	66	66	73	75
	90	58	58	64	68
	92	55	55	60	64

https://doi.org/10.52202/069179-0105

Again for a relative yield of 85%, the predictor VB+Edyn,log was able to produce 109 T14 boards; here, the trade-off was 10 fewer T14 boards and 11 fewer reject boards, which is considerably more efficient.
At the same level of relative yield, the perfect prediction traded 7 fewer T14 boards against 10 fewer reject boards.
At the highest relative yield level in Table 1 (92%), VB and VB+FE only led to a production of 83 T14 boards, VB+Edyn,log to a production of 89 T14 boards, and the perfect prediction to a production of 96 T14 boards.

4 CONCLUSIONS

In this study, data from log scanning were successfully used to predict the yield of the final strength grading of dried sawn timber. The input data were based on images from log computed tomography (CT) and dynamic modulus of elasticity of the log. As an additional input to the yield prediction models, a Finite Element analysis based on the CT images and using simulated fibre orientations was performed.
Based on these yield predictions, a pre-sorting strategy was tested where only logs with high predicted yield in the strength grade T14 were directed towards producing machine strength graded timber.
Using this approach, the T14 grade yield at the sawn timber strength grading process step could be increased from 80% to up to 92%, at the cost of losing up to 30% of the T14 boards which could have been produced if all of the logs in the study had been sent to the strength grading process.
Although the results on Young's modulus from Finite Element analysis had a coefficient of determination of 0.46 with the tensile modulus of elasticity, using this result for predicting the strength grading yield did not improve the pre-sorting efficiency.
Further research should be directed towards increasing the accuracy of the Finite Element analysis, e.g. by basing it on a three-dimensional board grid instead of a two-dimensional board grid. It is also expected that a better prediction of the density of the dry board from the CT images could improve the accuracy of the Finite Element analysis.

ACKNOWLEDGEMENT

The research for this study was part of the project READiStrength, which was funded by the ERA-NET Cofund Call "ForestValue – Innovating the forest-based bioeconomy" as well as by the national funding agencies Vinnova, Fachagentur Nachwachsende Rohstoffe e.V. and the Austrian Federal Ministry for Agriculture, Regions and Tourism.

REFERENCES

[1] European Commission. Innovating for sustainable growth: A bioeconomy for Europe. Luxembourg: Publications Office of the European Union 2012.
[2] Hintsteiner WJ, van Loo M, Neophytou C, Schueler S, Hasenauer H. The geographic origin of old Douglas-fir stands growing in Central Europe. Eur J Forest Res 2018; 137(4): 447–61.
[3] Sauter UH. Technologische Holzeigenschaften der Douglasie als Ausprägung unterschiedlicher Wachstumsbedingungen: [Technical Douglas fir wood properties as an effect of different growing conditions] Dissertation thesis. University of Freiburg 1992.
[4] Rais A, Poschenrieder W, Pretzsch H, van de Kuilen J-WG. Influence of initial plant density on sawn timber properties for Douglas-fir (Pseudotsuga menziesii (Mirb.) Franco). Ann For Sci 2014; 71(5): 617–26.
[5] Johansson E, Johansson D, Skog J, Fredriksson M. Automated knot detection for high speed computed tomography on Pinus sylvestris L. and Picea abies (L.) Karst. using ellipse fitting in concentric surfaces. Comput Electron Agr 2013; 96: 238–45.
[6] CEN European Committee for Standardization. EN 408:2012. Timber structures – Structural timber and glued laminated timber – Determination of some physical and mechanical properties. EN 408:2010+A1:2012-07. Brussels; 2012.
[7] CEN European Committee for Standardization. EN 384:2018. Structural timber – Determination of characteristic values of mechanical properties and density. EN 384:2015+A1:2018. Brussels; 2018.
[8] Smith RGB, Palmer G, Davies M, Muneri A. A method enabling the reconstruction of internal features of logs from sawn lumber: The log end template. Forest prod j 2003; 53(11-12): 95–8.
[9] R Core Team. R: A Language and Environment for Statistical Computing. Vienna, Austria; 2020. Available from: https://www.R-project.org/.
[10] Chang W, Cheng J, Allaire JJ, Xie Y, McPherson J. shiny: Web Application Framework for R; 2020. Available from: https://CRAN.R-project.org/package=shiny.
[11] Huber JAJ, Broman O, Ekevad M, Oja J, Hansson L. A method for generating finite element models of wood boards from X-ray computed tomography scans. Comput Struct 2022; 260(2): 106702.
[12] COMSOL Multiphysics® v. 6.0. Stockholm, Sweden: COMSOL AB. Available from: www.comsol.com/.
[13] Dinwoodie JM. Timber: Its Nature and Behavior. 2nd ed., revised. New York, Florence: Spon Press [Imprint]; Routledge; Taylor & Francis Group [distributor] June 2000.
[14] CEN European Committee for Standardization. EN 14081-2:2018. Timber structures – Strength graded structural timber with rectangular cross section – Part 2: Machine grading; additional requirements for type testing. Brussels; 2018.
[15] CEN European Committee for Standardization. EN 338:2016. Structural timber – Strength classes. Brussels; 2016.
[16] CEN European Committee for Standardization. EN 14080:2013. Timber structures - Glued laminated

https://doi.org/10.52202/069179-0105

timber and glued solid timber - Requirements. Brussels; 2013.
[17] Wickham H. ggplot2: Elegant graphics for data analysis. Second edition. Cham: Springer International Publishing 2016.
[18] Olsson A, Pot G, Viguier J, Hu M, Oscarsson J. Performance of timber board models for prediction of local bending stiffness and strength - with application on douglas fir sawn timber. Wood Fiber Sci 2022; 54(4): 226–45.
[19] Denzler JK, Weidenhiller A. Pre-grading of spruce logs containing frozen and unfrozen water by means of frequency-based nondestructive testing (NDT). Holzforschung 2016; 70(1): 79–85.